Ann. Geophys., 26, 2303–2309, 2008
www.ann-geophys.net/26/2303/2008/

Annales Geophysicae

The EISCAT meteor code

G. Wannberg[1], **A. Westman**[2], **J. Kero**[1], **C. Szasz**[1], **and A. Pellinen-Wannberg**[3]

[1]Swedish Institute of Space Physics, P.O. Box 812, 981 28 Kiruna, Sweden
[2]EISCAT Scientific Association, P.O. Box 812, 981 28 Kiruna, Sweden
[3]Umeå University and Swedish Institute of Space Physics, P.O. Box 812, 981 28 Kiruna, Sweden

Received: 20 December 2007 – Revised: 13 May 2008 – Accepted: 10 June 2008 – Published: 5 August 2008

Abstract. The EISCAT UHF system has the unique capability to determine meteor vector velocities from the head echo Doppler shifts measured at the three sites. Since even meteors spending a very short time in the common volume produce analysable events, the technique lends itself ideally to mapping the orbits of meteors arriving from arbitrary directions over most of the upper hemisphere.

A radar mode optimised for this application was developed in 2001/2002. A specially selected low-sidelobe 32-bit pseudo-random binary sequence is used to binary phase shift key (BPSK) the transmitted carrier. The baud-length is 2.4 μs and the receiver bandwidth is 1.6 MHz to accommodate both the resulting modulation bandwidth and the target Doppler shift. Sampling is at 0.6 μs, corresponding to 90-m range resolution. Target range and Doppler velocity are extracted from the raw data in a multi-step matched-filter procedure. For strong (SNR$>$5) events the Doppler velocity standard deviation is 100–150 m/s. The effective range resolution is about 30 m, allowing very accurate time-of-flight velocity estimates. On average, Doppler and time-of-flight (TOF) velocities agree to within about one part in 10^3. Two or more targets simultaneously present in the beam can be resolved down to a range separation $<$300 m as long as their Doppler shifts differ by more than a few km/s.

Keywords. Electromagnetics (Plasmas; Signal processing and adaptive antennas) – Ionosphere (Instruments and techniques)

1 The first ten years of EISCAT meteor observations

Meteor head echoes were first detected at EISCAT during the Geminid meteor shower in December 1990, when transient, multiply-peaked radar echoes from altitudes around 100 km were seen in power profile data from a high-resolution UHF experiment using a (13$\times$3 μs) Barker coded binary phase-shift keying (BPSK) for pulse compression and very wide post-detection filter bandwidths. Nobody at EISCAT had seen anything like these echoes before, and experienced users suggested that they were artefacts caused by an equipment malfunction. However, when it was demonstrated by computer simulations that the observed echo shapes could be replicated by passing strongly Doppler-shifted signals through a matched filter set for zero Doppler, the events were accepted as genuine and echoes off meteor heads suggested as the most plausible explanation (Pellinen-Wannberg and Wannberg, 1994).

A comprehensive analysis of the EISCAT receiver system and its response to Doppler shifted Barker-coded echoes was now performed and a time-slicing correlator code and techniques for inverting the observed power domain ambiguity functions into target velocities were developed by Wannberg et al. (1996). From 1993 to 1999, a radar mode based on this work but employing a (13$\times$2 μs) Barker coded pulse was used to accumulate a database that eventually yielded the first tristatic high-power large aperture (HPLA) radar meteor vector velocities and ephemerides (Janches et al., 2002a, b).

The unity-SNR radar cross section (RCS) sensitivity of the (13$\times$2 μs) waveform, as implemented on the old signal processing system and used in nearly all pre-2001 measurements, is -65 dB m^2 at UHF and 100-km range. At VHF it is -70 dB m^2. This is assuming perfect pulse-compression. In practice, since the Doppler-shifted signal from a fast-moving meteor target causes the echo power to spread over several range gates, the effective sensitivity is reduced to about -58 dB m^2 at UHF and -63 dB m^2 at VHF. These numbers are at least 7–10 dB inferior to what complex-amplitude domain data processing could have achieved, but hardware limitations in the correlator and the data recording system made this a practical impossibility at the time (Wannberg et al., 1996). It was only after the installation of the new digital

Correspondence to: G. Wannberg
(ugw@irf.se)

Published by Copernicus Publications on behalf of the European Geosciences Union.

Table 1. Geometry of the EISCAT UHF 2002 meteor velocity mode. The common observation volume is located at (68.876 N, 21.880 E) at 96.0 km altitude.

Site	Distance to common volume (km)	Elevation angle (degrees)	Scattering angle (degrees)	$\boldsymbol{k}$ vector angle relative to $\boldsymbol{k}_T$ (degrees)
Tromsø	163.6	35.3	180.0	0.0
Kiruna	160.4	36.0	104.4	37.8
Sodankylä	278.5	18.9	57.8	61.1

signal processing and raw data recording systems in 2001 that phase-coherent pulse-by-pulse analysis could finally be applied. At that point, the development of an optimised radar mode, making full use of the capabilities of the new hardware, was started.

2 The new post-2001 meteor mode

2.1 Pointing geometry

In the UHF frequency range, scattering of EM waves off a compact ball of plasma, e.g. the plasma cloud accompanying a meteoroid interacting with the atmosphere, is essentially elastic. When such a target scatters an incident wave with frequency f_0 and wave vector $\boldsymbol{k}_0$ into a secondary wave with frequency f_1 and wave vector $\boldsymbol{k}_1$, it contributes a wave vector

$$\boldsymbol{k} = (\boldsymbol{k}_1 - \boldsymbol{k}_0) \tag{1}$$

in order for momentum to be conserved. If the target is moving with velocity $\boldsymbol{v}$, the scattered wave is Doppler-shifted by an amount f_D proportional to the component of $\boldsymbol{v}$ along $\boldsymbol{k}$, such that to first order

$$\boldsymbol{v} \cdot \boldsymbol{k} = f_D/|\boldsymbol{k}| \tag{2}$$

When the EISCAT UHF system is used for tristatic meteor head echo observations, the Doppler shift of the scattered signal received at Tromsø is therefore proportional to the component of target velocity along the Tromsø antenna line-of-sight (i.e. the classical monostatic backscatter case), while the Doppler shifts simultaneously observed at Kiruna and Sodankylä are proportional to the velocity components directed along the bisectors of the Tromsø-Kiruna and Tromsø-Sodankylä scattering angles, respectively. Similarly, changes in target range observed at the three sites reflect the components of target motion along the respective scattering vectors and can be used to estimate the three velocity components by the time-of-flight method. As the scattering geometry is defined by the radar system configuration and the antenna pointing, and therefore known, it is then straightforward to construct the full target vector velocity at the scattering location.

Unfortunately, the UHF system geometry is far from ideal for high-precision vector velocity measurements when the system is used in the "conventional" manner, i.e. with the Tromsø beam directed either tangential to the magnetic field or vertically (the latter being almost mandatory for experiments attempting to observe plasma processes in the D and E regions). Since the Sodankylä station is located more or less southeast of Tromsø, and the Kiruna station due south, the velocity components derived in Kiruna and in Sodankylä in this configuration end up being strongly linearly dependent (Janches et al., 2002a).

However, since the primary application foreseen for the new experiment – a meteor sky survey – does not demand background ionospheric data, it was decided to select a pointing geometry minimising the linear dependence of the measured velocity components. By fixing the beam intersection point at (68.876° N, 21.880° E, altitude 96.0 km), almost in the Tromsø – Sodankylä plane and chosen such that the distances to the Tromsø and Kiruna receivers are close to equal, the three scattering $\boldsymbol{k}$-vectors are spread nearly as far apart as possible within the restrictions set by the system geometry. At the same time, the size of the common volume (and thus indirectly the event rate) is increased by almost a factor of two relative to the earlier, vertical-above-Tromsø geometry. The Sodankylä beam elevation is increased to 18.9 degrees, so essentially eliminating ground noise pickup.

Details of the meteor mode geometry can be found in Table 1. With minor modifications, this geometry has been used for all UHF meteor observations after 2001, see reported results in Kero et al. (2008a, b, c), Szasz et al. (2007) and Szasz et al. (2008).

2.2 The radar code

One of the most serious shortcomings of the power-domain meteor radar code was its inability to provide unambiguous velocity estimates all the way up to the maximum apparent solar system escape velocity, 72 km s^{-1} – the Barker power-domain response wraps around at about 36 km s^{-1} and so additional assumptions had to be invoked whenever it was unclear if a particular event was below or above the wraparound velocity (Wannberg et al., 1996). To rectify this and at the same time make sure that the new experiment would be able to resolve even the fastest (possibly interstellar) meteors, it would have to be designed to provide unambiguous Doppler velocity estimates up to and exceeding 100 km s^{-1}, paired with a line-of-sight velocity resolution better than 150 m s^{-1} over the whole velocity range.

Since some of the old data contained features suggesting that the Doppler velocity measurements might be slightly negatively biased, possibly indicative of a continuous slipping of the plasma produced in the meteoroid-atmosphere interaction, it was also considered essential to keep the pulse

repetition rate as high as possible to permit reliable comparative time-of-flight velocity measurements to be made (Pellinen-Wannberg et al., 1998). But at the same time, this would need to be reconciled with the requirement that the experiment should deliver the best possible rate of statistics and maximum ionospheric clutter suppression, as well as with the additional restriction that the experiment should provide mono-static range coverage over at least 120 to 155 km to match the optimised 3-static UHF geometry described above.

The above considerations were now translated into some basic design criteria:

- The receiver bandwidth should be at least 1.5 MHz to accommodate both the modulation bandwidth and the target Doppler shift,
- Accordingly, the complex-valued receiver output voltage should be sampled at 1.5 Msamples s^{-1} or faster,
- The sampled data should be recorded on a pulse-by-pulse basis to enable subsequent amplitude-domain processing,
- Frequency hopping on alternate pulses should be employed to minimise ionospheric F region clutter, and
- The pulse repetition rate should fall in the (400...800) Hz range, corresponding to a radar cycle length of (1.25...2.5) ms.

At this point it became apparent that the restrictions on the radar cycle length, combined with the maximum allowable RF duty cycle of the transmitter, 10%, would limit the longest permissible transmission to something in the order of 125 μs. This meant that the desired 150 m s^{-1} velocity resolution could not be achieved on a single radar cycle basis, as this would require the target to be illuminated for a millisecond or more, thus overlapping part or the entire desired reception time window. Instead, accurate velocity estimates would have to be derived from fitting a time-dependent polynomial (target range, velocity, deceleration) model to a series of data observed on successive radar pulses, and it was decided to design and validate a data reduction scheme optimised to the radar waveform in parallel to the design of the actual experiment.

At the time, reliable observational data on the spatial and temporal development of the plasma behind a meteoroid was still scarce, mainly because the spatial resolution and dynamic range of previous experiments had been much too poor to resolve the head echo and a possible simultaneous, much weaker return from the plasma tail. To improve on this situation, it was decided that the new meteor mode should employ a modulating waveform with a baud-length in the order of 2 μs, the shortest pulse compatible with both the UHF and the VHF transmitter characteristics (the instantaneous power bandwidth of the VHF klystrons is too narrow to replicate 1 μs pulses, which are stretched and rounded such that the effective output pulse length becomes more like 1.5 μs). Its range ambiguities should be suppressed by more than −30 dBmax within ±1 km from the desired range response, and by at least −15 dBmax elsewhere. With such a code, it should be possible to resolve returns from slipping plasma separated from the head echo by as little as a single baud-length.

In the EISCAT transmitter system, the transmitted waveform is generated by applying binary ($0/\pi$) phase modulation (also known as BPSK) to the carrier frequency. The waveform is therefore conveniently defined in terms of binary (0,1) sequences of arbitrary length. In the present case, either a 64-bit sequence or two 32-bit sequences could be used to generate the maximum permissible RF pulse length, assuming a baud-length of 2 μs.

Since the normalised side-lobe level of the autocorrelation of an n-bit pseudo-random sequence is something between n^{-1} and n^{-2} (Cook et al., 1975), there was a good chance that there existed a 32-bit sequence that would meet the −30 dBmax close-in range ambiguity requirement. Making use of the fact that mirror symmetry exists between a [0, x_n] code and a [1, x_n^{-1}] code – their autocorrelation functions are identical – a Matlab algorithm was designed to find those binary sequences from 1 to 2^{31} meeting the condition

$$[r_{xx}(k,i)]^2 < 10^{-3}[r_{xx}(k,0)]^2, i = 1...3 \quad (3a)$$

where $r_{xx}(k,i)$ is the autocorrelation of code k at an offset of i bauds from the origin. For each k=κ representing a sequence meeting Eq. (3a), the total sidelobe power $P_S(\kappa)$ is computed and compared to the previous best value:

$$P_S(\kappa) = 2\Sigma[r_{xx}(\kappa,i)]^2, i = 1,...,31, \quad (3b)$$

if

$$P_S(\kappa) < \inf_{k=(1...\kappa-1)}\{P_S\} \text{ then } \inf\{P_S\} = P_S(\kappa) \text{ and } \kappa_{\text{opt}} = \kappa \quad (3c)$$

At any given point in the search, κ_{opt} thus represents the best code found so far.

Having tested only about 10% of all 32-digit permutations, the algorithm came up with the sequence

$$00000001010010101110001100100110 \quad (4)$$

As shown in Fig. 1, its range ambiguities over the first three gates either side of the central peak are all below −30 dBmax and the worst-case ambiguities at plus and minus four gates are below −17 dBmax. About 88% of the total power is contained in the central peak. The power frequency spectrum is shown in Fig. 2. Since the experiment design work was done under time pressure and this sequence met our requirements, it was immediately selected as the modulating waveform. Purely by chance it also proved to be the best of all 32-digit sequences, given our search criteria; a later, exhaustive search using a highly optimised C program did not come up with any better sequence.

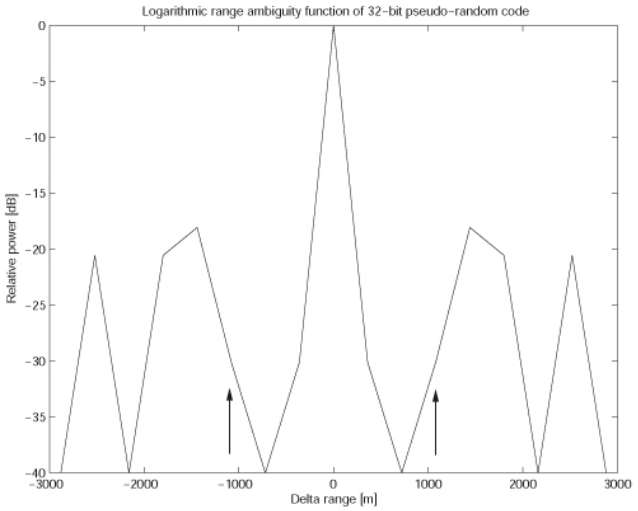

Fig. 1. Normalised logarithmic range ambiguity (autocorrelation) of the 32-bit sequence (4) defining the transmitted waveform, assuming a 2.4 μs baud-length. The central peak is surrounded by a region out to plus and minus three bit intervals (indicated by the arrows) where the response is down by more than −30 dB.

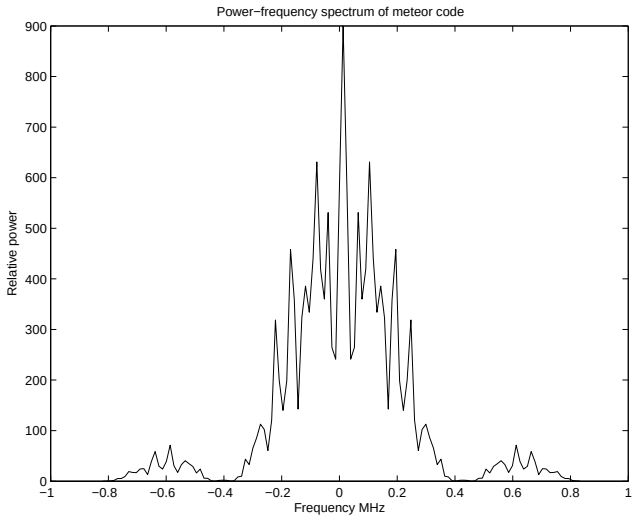

Fig. 2. Power frequency spectrum (PFS) of sequence (4) assuming a 2.4 μs baud-length.

A schematic representation of the basic radar cycle designed on the basis of the above deliberations is given in Fig. 3. Two RF pulses are transmitted. The first of these is normally received at all three sites. Sequence (3) is BPSK modulated onto the transmitter carrier using a 2.4 μs baud-length, for a total pulse length of 76.8 μs. The transmission is frequency-hopped between two different carrier frequencies F5 and F9 (927.5 MHz and 928.7 MHz) on alternate pulses to place the first ambiguous range well above the F region peak at more than 600 km altitude, so minimising contamination of the mono-static data by incoherent returns from the ionospheric F-region. To improve the utilisation of the available klystron beam power, the waveform is then repeated on F12 (929.6 MHz) for the benefit of the remote receivers. In this way, an RF duty cycle approaching 10% can be maintained.

Unfortunately, the radio-frequency interference situation at Sodankylä sometimes forces the insertion of a 1.5 MHz wide (929.0–930.5) front-end filter into the signal path to protect the receiver from being overloaded by the strong carriers from GSM mobile telephone base stations operating just above 935 MHz, thus effectively ruling out the possibility of receiving the F5/F9 transmissions there.

The scattered signals are received at all three UHF sites. The receiver −3 dB bandwidth is set to 1.6 MHz to accommodate the combined effect of modulation bandwidth and target Doppler shift. The sampling interval is 0.6 μs, corresponding to a sampling frequency of 1.6667 MHz and 90-m range resolution.

This radar mode has a unity-SNR RCS sensitivity of $-78.5\,\mathrm{dB\,m^2}$ at UHF and 100-km range, which represents a dramatic performance improvement of almost 20 dB relative to the pre-2001 power-domain code. It can also be used on the VHF system; its sensitivity is then $-83.5\,\mathrm{dB\,m^2}$. The basic experiment exists in several versions, which differ mainly in the length of the radar cycle. Except for in the very first runs, this is always chosen to be an integer multiple of the baud-length.

3 Data reduction

Target range and Doppler frequency are extracted from the recorded complex amplitude data in a multi-step matched-filter procedure. To locate the first point of an echo in the range/time domain, a signal power vs. range function is computed from the complex amplitude data and convolved with a normalised power-domain model of an infinite-SNR echo – essentially a 128 samples long boxcar function. The convolution is an efficient averaging operation, the result of which shows a distinct peak at a fixed offset relative to the leading edge of an echo when the boxcar model overlaps it exactly. However, the weakest echoes are so noisy that just picking the maximum values of the resulting convolutions does not give a reliable indication of the echo positions. A second step of averaging is therefore applied by convolving the result of the first convolution operation with the convolution of the model echo with itself – a 256 samples long triangular function. Picking the maximum value of this second convolution typically fixes the first point of an echo – or equivalently, the range to the target – to within one or two samples in the data vector. Starting from that position, a 128-sample subset of the amplitude data vector is Fourier transformed and its power frequency spectrum convolved with the normalised theoretical power frequency spectrum of the transmitted pulse. Again, noisy experimental data frequently

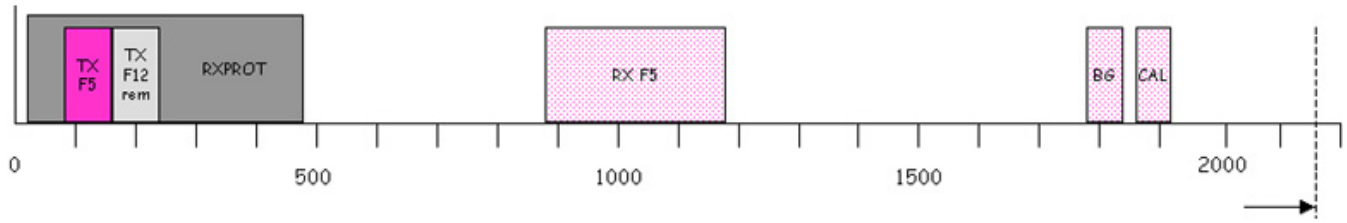

Fig. 3. Schematic representation of a basic monostatic radar cycle. Time is in units of microseconds. The transmission intended for reception at all sites alters between EISCAT frequencies F5 and F9, the transmission for the remote receivers occurs at F12. BG and CAL denote sampling intervals dedicated to background estimation and system calibration.

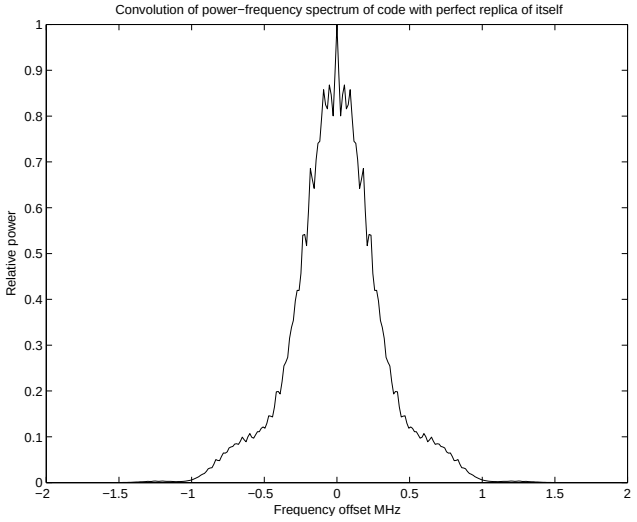

Fig. 4a. Convolution of the theoretical PFS of sequence (4) with an infinite-SNR radar echo from a hard target (e.g. a meteor head echo).

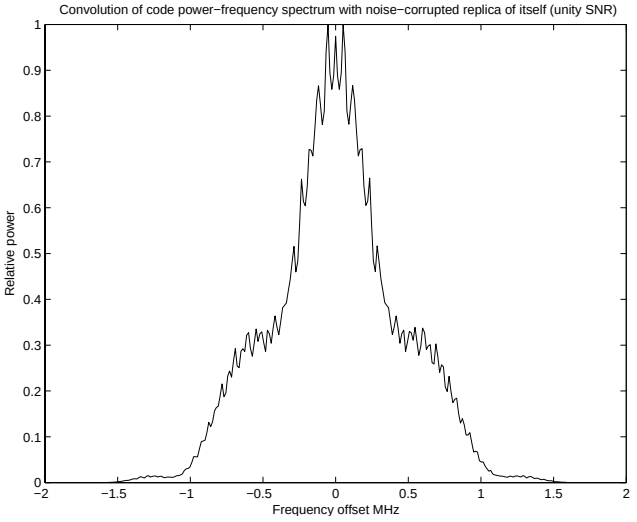

Fig. 4b. Convolution of the theoretical PFS of sequence (4) with a unity-SNR radar echo from a hard target (e.g. a meteor head echo). Note that even at this very high SNR the noise-induced variance of the signal can generate spurious peaks in the convolution; the data reduction routine therefore uses the centre of gravity of the convolution as the first estimate of the Doppler shift.

causes this convolution to be multi-peaked, such that its maximum cannot be used as a reliable estimate of Doppler shift (Fig. 4a and b). Instead, the frequency of its centre of gravity is taken as the first Doppler estimate.

Finally, the range and Doppler estimates are input to a time-domain fine-tuning procedure. A model of the received signal is constructed by generating a complex sinusoid at the estimated Doppler frequency and BPSK-modulating it by a range-shifted replica of the pseudo-random code. The raw data vector is cross-correlated with the model and the pulse compression ratio computed from the correlation function. A robust gradient-search routine then varies range and Doppler in small steps until the compression ratio maximises and their values at maximum are taken as the best estimates. When applied to strong (SNR>5) events, the best compression ratio typically exceeds 80%. A detailed description how the fitting procedure is performed in practice is given in Kero et al. (2008c).

4 A case study – a dual target event observed with the VHF system

The data reduction procedure described above is designed to work automatically, assuming there is only one dominant target in the beam at any time. Given the relatively low incidence rate of head echoes, this is normally the case and the procedure converges nicely. In the very unlikely event that two or more targets are in the beam simultaneously, manual intervention is required to sort things out. The mono-static VHF data presented in Fig. 5 shows a beautiful case in point. Here we have two targets, well separated in the Doppler domain but so close in range that they are both almost fully illuminated by the 76.8 μs pulse. Each of the two Doppler peaks is compressed to about 41%, indicating that the two targets have nearly equal radar cross sections and contribute equally to the echo power. A full range-Doppler decoding

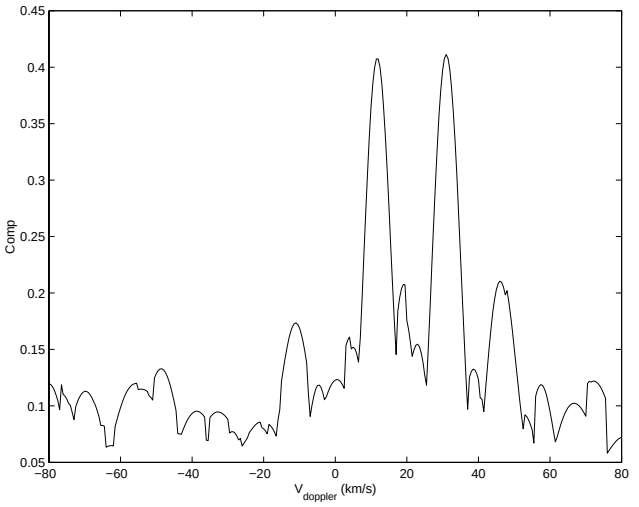

Fig. 5. Pulse compression ratio as function of the Doppler velocity for a dual target VHF event. Two unrelated targets, so close to each other in range that they are both almost fully illuminated, are well resolved in the Doppler domain. Each of the two Doppler peaks is compressed to about 41%, indicating that at this particular range, the two targets contribute about equally to the echo and therefore must have very similar radar cross sections.

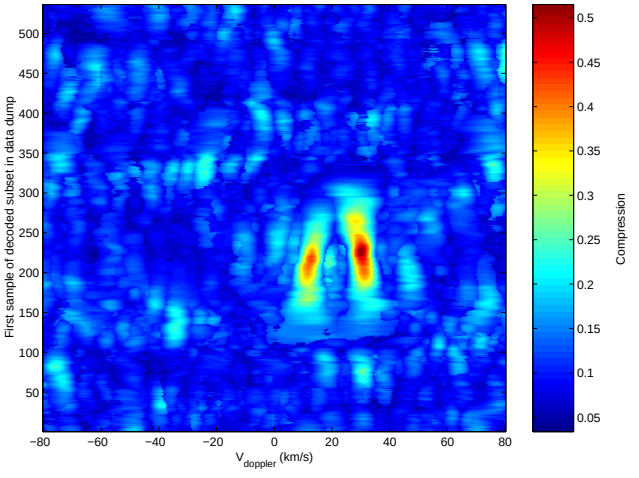

Fig. 6. A full range-Doppler decoding of the same sample vector shows that the two targets are actually separated in range by about 670 m, i.e. slightly less than two code bits.

of the same sample vector (Fig. 6) shows that at this point in time the two targets are actually separated in range by about 670 m, i.e. slightly less than two code bits.

This was a quite extended event, lasting for nearly 0.12 s. Both targets could be uniquely resolved both in range and in Doppler in more than 50 radar cycles. As shown in Fig. 7, they are clearly not associated with one another as their velocities differ by a factor of more than two and their trajectories actually cross each other at about 0.05 s. Note that the

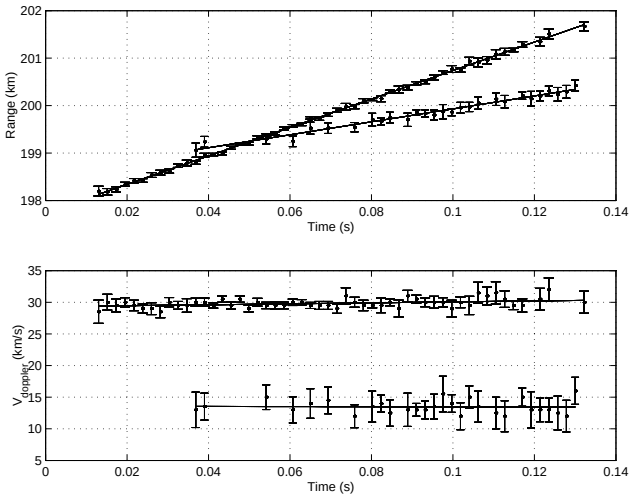

Fig. 7. The snapshots presented in Figs. 5 and 6 are taken from this extended event, which lasted for almost 0.12 s. Both targets are clearly distinguishable in more than 50 radar cycles. Linear least-squares fits of their positions and line-of-sight velocities clearly show that in this particular case the two targets are completely unrelated, even though they appear at the same range at approx. 55 ms into the event. At that point it is still possible to resolve them down to a separation distance of about 200 m.

two targets can still be clearly resolved when less than 200 m apart, corresponding to about one-half of a baud-length!

5 Results and conclusions

The new EISCAT meteor mode has been shown to achieve 100–150 m s^{-1} Doppler velocity standard deviation and an effective range resolution of about one-third of a range gate (30 m), so making it possible to generate very accurate time-of-flight velocity estimates with mean errors below 50 m s^{-1}; in favourable cases the errors can even approach 10 m s^{-1}. A statistical analysis of a database containing more than 410 tristatic events recorded and analysed by this technique (Fig. 8) shows the Doppler-derived velocities agreeing with those derived by the time-of-flight method to within about one part in 10^3 with negligible biases. This demonstrates that, to within the measurement accuracy, no contribution from slipping plasma can be detected and the Doppler velocities are in fact unbiased. Whether this is the result of there actually being very little plasma slipping backwards into the tail and surviving there, or a consequence of the signal from possibly existing plasma "tails" being too weak to be detectable above the receiver noise, cannot be determined; in any case the scattering cross section a few hundred metres down the trajectory is at least two orders of magnitude below that of the meteor head. Since the Doppler velocity measure is shown to be statistically indistinguishable from the time-of-flight one, even the orbital parameters and trajectories of

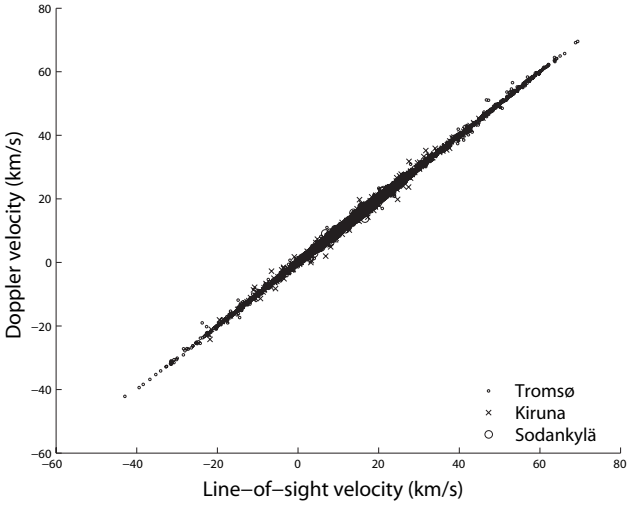

Fig. 8. Doppler velocity vs. time-of-flight velocity for 410 meteor events for which the two estimates differ by less than 5 km s^{-1}. Linear LMS fits to the data sets from the three stations yield the following:

Tromsø: v_D=1.0001 v_{TOF}–0.0155
Kiruna: v_D=0.9998 v_{TOF}–0.0180
Sodankylä: v_D=0.9987 v_{TOF}–0.0086.

meteoroids passing through one or more of the beams very rapidly can be determined reliably.

The EISCAT meteor mode as described, including radar code, observation geometry and data reduction procedure, is currently the de facto standard for all meteor work performed with the EISCAT mainland systems.

Acknowledgements. We gratefully acknowledge the assistance provided by the EISCAT staff during the experiments. EISCAT is an international research association supported by research organisations in China (CRIPR), Finland (SA), Germany (DFG), Japan (NIPR and STEL), Norway (NFR), Sweden (VR) and the United Kingdom (STFC). Two of the authors (J. Kero and C. Szasz) are financed by the Swedish National Graduate School of Space Technology.

Topical Editor K. Kauristie thanks J. Vierinen and another anonymous referee for their help in evaluating this paper.

References

Cook, C. E., Bernfeld, M., and Palmieri, C. A.: Matched Filtering, Pulse Compression and Waveform Design, in: Radars, vol. 3, Pulse Compression, edited by: Barton, D. K., Raytheon, Bedford, Mass., 1975.

Janches, D., Pellinen-Wannberg, A., Wannberg, G., Westman, A., Häggström, I., and Meisel, D. D.: Tristatic observation of meteors using the 930 MHz EISCAT radar system, J. Geophys. Res., 107(A11), 1389, doi:10.1029/2001JA009205, 2002a.

Janches, D., Pellinen-Wannberg, A., Wannberg, G., Meisel, D. D., Westman, A., and Häggström, I.: The tristatic 930 MHz EISCAT radar system: a unique tool for meteor/dust studies, URSI GA Proceedings, 2002b.

Kero, J., Szasz, C., Pellinen-Wannberg, A., Wannberg, G., Westman, A., and Meisel, D. D.: Three-dimensional radar observation of a submillimeter meteoroid fragmentation, Geophys. Res. Lett., 35, L04101, doi:10.1029/2007GL032733, 2008a.

Kero, J., Szasz, C., Wannberg, G., Pellinen-Wannberg, A., and Westman, A.: On the meteoric head echo radar cross section angular dependence, Geophys. Res. Lett., 35, L07101, doi:10.1029/2008GL033402, 2008b.

Kero, J., Szasz, C., Pellinen-Wannberg, A., Wannberg, G., Westman, A., and Meisel, D. D.: Determination of meteoroid physical properties from tristatic radar observations, Ann. Geophys., 26, 2217–2228, 2008c, http://www.ann-geophys.net/26/2217/2008/.

Pellinen-Wannberg, A. and Wannberg, G.: Meteor observations with the European incoherent scatter UHF radar, J. Geophys. Res., 99, 11 379–11 390, 1994.

Pellinen-Wannberg, A., Westman, A., Wannberg, G., and Kaila, K.: Meteor fluxes and visual magnitudes from EISCAT radar event rates: A comparison with cross section based magnitude estimates and optical data, Ann. Geophys., 16, 1475–1485, 1998, http://www.ann-geophys.net/16/1475/1998/.

Szasz, C., Kero, J., Meisel, D. D., Pellinen-Wannberg, A., Wannberg, G., and Westman, A.: Estimated visual magnitudes of the EISCAT UHF meteors, Earth, Moon, and Planets, 95, 101–107, doi:10.1007/s11038-007-9206-y, 2007.

Szasz, C., Kero, J., Meisel, D. D., Pellinen-Wannberg, A., Wannberg, G., and Westman, A.: Orbit characteristics of the tristatic EISCAT UHF meteors, Monthly Notices of the Royal Astronomical Society, MN-08-0446-MJ.R1, 2008.

Wannberg, G., Pellinen-Wannberg, A., and Westman, A.: An ambiguity-function-based method for analysis of Doppler decompressed radar signals applied to EISCAT measurements of oblique UHF-VHF meteor echoes, Radio Sci., 31, 497–518, 1996.